



Pergamon

Biorganic &amp; Medicinal Chemistry, Vol. 5, No. 6, pp 1185-1195, 1997

© 1997 Elsevier Science Ltd

All rights reserved. Printed in Great Britain  
0968-0896/97 \$17.00 + 0.00

PII: S0968-0896(97)00065-5

Exhibit 7

## Discovery of Selective, Small-Molecule Inhibitors of RNA Complexes—II. Self-Splicing Group I Intron Ribozyme

NOTICE: THIS MATERIAL MAY BE PROTECTED  
BY COPYRIGHT LAW (TITLE 17 U.S. CODE)

Houng-Yau Mei,\* Mei Cui, Shannon M. Lemrow and Anthony W. Czarnik<sup>†</sup>

BioOrganic Chemistry Section, Department of Chemistry, Parke-Davis Pharmaceutical Research, Division of  
Warner-Lambert Company, 2800 Plymouth Road, Ann Arbor, MI 48106, U.S.A.

**Abstract**—Self-splicing group I intron RNA was chosen as a potential therapeutic target for small-molecule intervention. High-throughput screening methodologies have been developed to identify small organic molecules that regulate the activities of these catalytic introns. Group I introns derived from pathogenic *Pneumocystis carinii* and phage T4 were used as model systems. Inhibitors identified from a library of  $\approx 150,000$  compounds were shown to regulate biochemical reactions including the two-step intron splicing and an RNA ligation catalyzed by the group I introns. These inhibitors provide a unique opportunity to understand small-molecule recognition of the self-splicing RNA. The methodologies developed for group I introns should be applicable to studies of other RNA systems. © 1997 Elsevier Science Ltd.

### Introduction

The findings of RNA catalysis in biological systems have not only revolutionized our thinking of the origin of life<sup>1</sup> but also stimulated significant research opportunities in drug discovery.<sup>2</sup> On one hand, RNA catalysts (ribozymes) can be used as therapeutic agents that target specific RNA sequences.<sup>3</sup> In principle, these ribozyme agents can be tailor-made to recognize (through Watson-Crick-like base-pairing) and to degrade (with their catalytic functions) any RNA targets. On the other hand, ribozymes can be regarded as one would any protein target whose functions can be regulated by therapeutic intervention.<sup>4</sup>

Group I intron RNA, identified in bacteriophages, fungi, algae, protozoa, and eubacteria but not in higher eukaryotes, represents one of the best-characterized ribozymes.<sup>5</sup> With magnesium and guanosine as cofactors, group I introns have been found to activate their own in vitro splicing in the absence of any proteins. Highly conserved secondary and tertiary structures of all known group I introns have been deduced from phylogenetic comparisons and molecular modeling.<sup>6</sup> The catalytic core of the group I introns is responsible for binding a guanosine cofactor and catalyzing a two-step splicing reaction (Fig. 1A). The mechanism of the in vitro self-splicing process (Fig. 1B), a 5'-cleavage reaction with guanosine and the re-ligation of the two exons, is universal for all group I introns even under in vivo conditions where certain proteins may be involved.<sup>7</sup> Group I introns and other classes of ribozymes<sup>8</sup> have been found in biologically relevant genes of several pathogenic microorganisms. Each class involves specific mechanisms of biocatalysis not likely found in humans.

It has been suggested that catalytic RNA could serve as a therapeutic target.<sup>4</sup> Molecules that regulate the splicing of group I intron-containing precursor RNA are suggested to affect the growth of the microorganisms containing these ribozymes.<sup>9</sup>

Nucleic acid or amino acid-based compounds<sup>10</sup> and metabolites such as streptomycin and other aminoglycoside antibiotics<sup>11</sup> have been demonstrated to inhibit in vitro self-splicing of group I introns. While these molecules represent the first examples of ribozyme inhibitors, there have been no reports of low molecular weight organic molecules that regulate the functions of catalytic group I introns.<sup>12</sup> We report here methodologies, including high-throughput screening assays, for the rapid identification of low molecular weight organic modulators of group I intron-related ribozymes. Regulation of the biochemical reactions catalyzed by group I introns obtained from *Pneumocystis carinii*<sup>13</sup> and a self-assembled ribozyme system derived from the self-splicing intron *SunY* of bacteriophage T4<sup>14</sup> will be discussed.

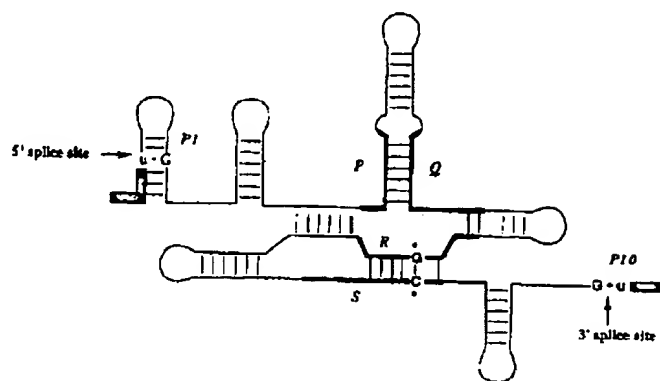
### Results and Discussion

#### Self-splicing group I introns in *Pneumocystis carinii*

*Pneumocystis carinii*, a yeast-like fungus, represents one of the most common infectious agents for immunocompromised patients.<sup>15</sup> In *P. carinii*, all copies of chromosomal genes of small subunit ribosomal RNA contain group I introns.<sup>13</sup> The splicing reactions are believed to be crucial in the maturation process of the biologically important *P. carinii* rRNA. A reconstructed precursor RNA molecule (552 nucleotides (nt) long) containing *P. carinii* group I intron (390 nt) and two short exon fragments (shown in Fig. 2A) is used as our

<sup>†</sup>Present address: IRORI Quantum Microchemistry, 11025 North Torrey Pines Road, La Jolla, CA 92037-1030, U.S.A

A



B

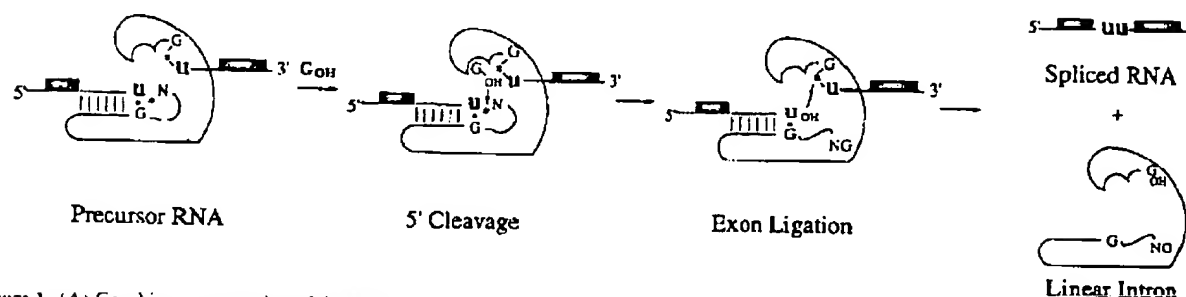


Figure 1. (A) Graphic representation of the secondary structure of the group I intron RNA. The arrows indicate the 5'- and 3'-splice sites which are situated around the P1 and P10 domains of the group I intron RNA, respectively. Heavy lines indicate the conserved secondary structure of the catalytic core domain (designated as P, Q, R, and S). The GC base pair (marked with asterisks) located in this core region is responsible for specific interaction with the guanosine cofactor for the self-splicing reactions. (B) The general mechanism of a two-step splicing reaction catalyzed by group I introns. In the presence of  $Mg^{2+}$ , a guanosine bound to the catalytic core activates the 5'-cleavage reaction at a specific phosphodiester linkage (\*) following a uridine residue (u). The released 5'-exon is then ligated to the 3'-exon by using its 3'-OH group to attack the 3'-spliced site (\*) usually followed by another uridine residue (u). The final products are a spliced RNA (ligated exons) and a linear intron.

model system. Figure 2(A) shows the two-step splicing reactions of this precursor RNA catalyzed by the *cis*-acting group I intron in the presence of a cofactor (guanosine or 5'-phosphorylated guanosine) and divalent cations such as  $Mg^{2+}$ . In the given example, the starting materials are full-length pre-rRNA (552 nt) and guanosine 5'-triphosphate (GTP). The products of the first cleavage reaction are two intermediate RNA fragments; a 113-nt RNA containing the 5'-exon and a guanosine-incorporated 439-nt RNA consisting of both the group I intron (390 nt) and the 3'-exon. The splicing reaction usually proceeds beyond the first step and the products from the second step include a ligated 5'- and 3'-exon (162 nt) and a released group I intron (390 nt) with a guanine residue at the 5'-end.<sup>16</sup>

Under *in vitro* conditions, splicing reactions occurred spontaneously in the transcription buffer (containing both GTP and  $Mg^{2+}$ ) required for synthesizing the precursor RNA. Figure 2(B) shows the desired products of the *in vitro* transcription; a full-length precursor RNA, accompanied by the spliced products. Interestingly, the full-length precursor RNA recovered from gel purification can still undergo self-splicing reactions in the absence of any protein enzymes. In Figure 2(B), lane 2 represents the self-splicing reactions

of a 5'-end labeled, full-length precursor RNA in the presence of  $Mg^{2+}$ . Self-splicing was initiated by the addition of guanosine cofactors. After self-splicing reactions, the samples were electrophoresed on a polyacrylamide gel. Out of the four possible RNA products, only the two shorter RNA fragments were radioactively labeled and visible on imaging the gel. The 113-nt RNA fragment represents 5'-exon released from the first splicing reaction and the 162-nt RNA represents the ligated exons as a result of a second splicing reaction. Lane 3 represents similar reactions on a nonradioactive precursor RNA with  $\alpha\text{-}^{32}\text{P}$  GTP as the cofactor. In contrast to reactions on the 5'-labeled precursors, only the two longer RNA products (5'- $^{32}\text{P}$  439-nt RNA from the 5'-cleavage reaction and 5'- $^{32}\text{P}$  390-nt RNA from the ligation reaction) are observed. These results indicate that in the presence of  $Mg^{2+}$  and guanosine, the folding process and the catalytic functions of group I introns are self-promoted with high efficiency.

We have developed a high-throughput screening assay for self-splicing group I introns using 96-well microtiter plates. The splicing reaction is initiated by the addition of  $\alpha\text{-}^{32}\text{P}$ -labeled GTP to a solution of nonradioactive precursor RNA. As indicated in Figure 2(A), the  $^{32}\text{P}$ -

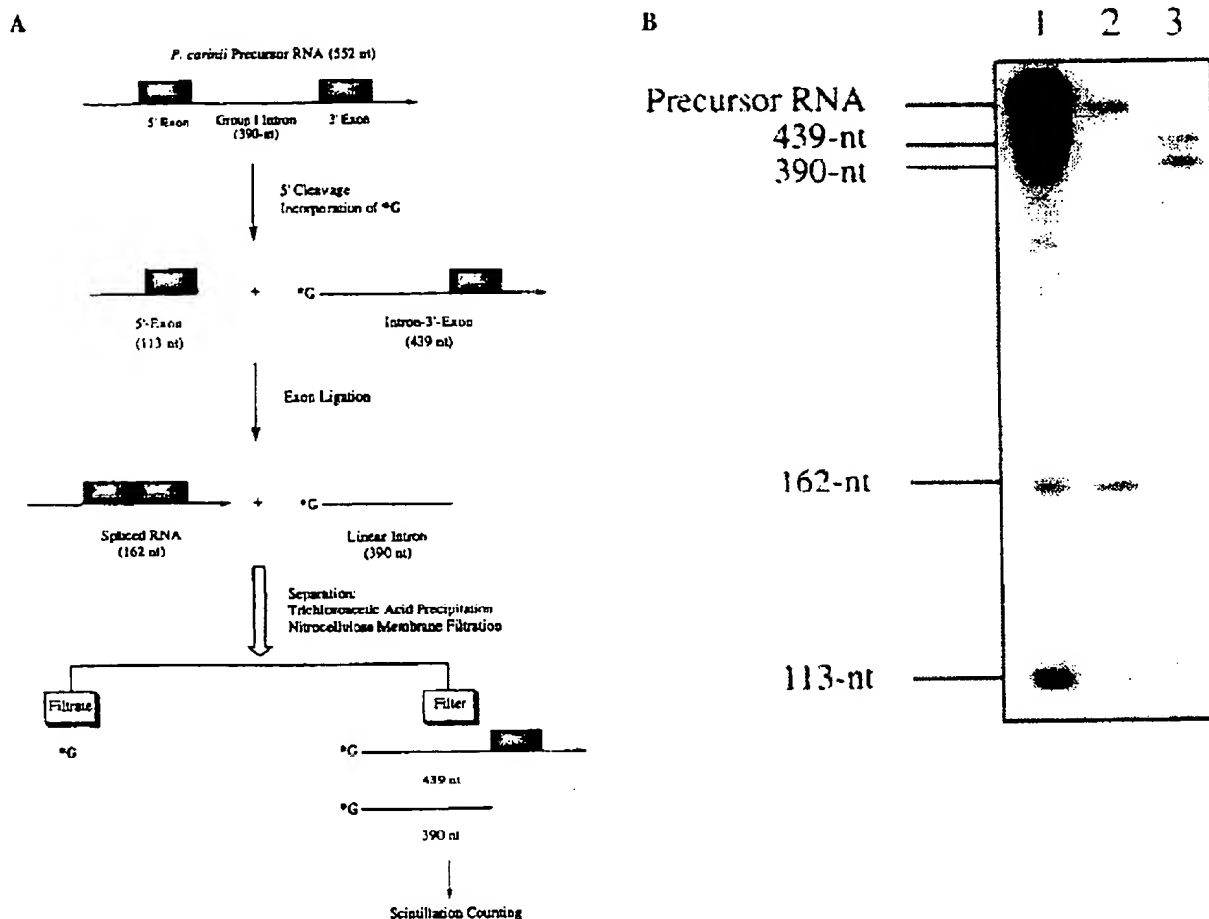


Figure 2. (A) In vitro self-splicing of a precursor RNA derived from *P. carinii* Ss-rRNA. All precursor RNA transcripts contain a 5'-exon and a 3'-exon interrupted by a group I intron. RNA self-splicing in *P. carinii* follows the same mechanism as described in Figure 1(B). In this example,  $^{32}\text{P}$ -G represents  $\alpha$ - $^{32}\text{P}$ -GTP which can be separated from  $^{32}\text{P}$ -G-439-nt and  $^{32}\text{P}$ -G-390-nt RNA products using TCA precipitation and a filtration procedure using nitrocellulose filters. The radioactivity retained on the filters is determined by scintillation counting. This value indicates the extent of self-splicing reactions. (B) Gel electrophoresis data of the synthesis and the self-splicing reactions of precursor RNA. Lane 1 shows the products of the precursor RNA synthesis using T7 in vitro transcription. In addition to the desired full length RNA, spliced products of 439-nt and 113-nt from the first step and 390-nt and 162-nt RNA from the second step are evident. Lane 2 represents the self splicing reactions of a purified 5'-end labeled precursor RNA. Spliced products from both steps (113-nt and 162-nt) are evident. Lane 3 shows the self-splicing reactions of a nonradioactive precursor RNA activated by the addition of  $^{32}\text{P}$ -GTP. The two desired products (439-nt and 390-nt) from both steps were observed.

labeled products of the two-step splicing reactions are 439-nt RNA and 390-nt RNA. Free GTP and the acid-precipitable longer RNA products can be readily separated using trichloroacetic acid (TCA) precipitation and subsequent filtration through a nitrocellulose membrane. The amount of radioactivity retained on the filter membrane represents the extent of the self-splicing reactions. This value obtained in the absence of any compounds (positive control experiments) is used as a reference for determining the efficacy of inhibition. If the first 5'-cleavage reaction is inhibited by added compounds, incorporation of  $^{32}\text{P}$ -GTP to the precursor RNA will be inhibited and a decreased amount of radioactivity will be found on the membrane.

A typical example of the results obtained from this high-throughput assay is shown in Figure 3. Figure 3(A)

shows the raw data (radioactivity in counts per million, cpm) of the self-splicing reactions performed on a 96-well microtiter plate. Column 1 represents the results of eight repeats of the self-splicing reactions in the absence of any inhibitors while column 12 represents the data of eight repeats of solution containing  $^{32}\text{P}$ -GTP only. Other control experiments such as self-splicing in the absence of  $\text{Mg}^{2+}$  or self-splicing reaction at time zero showed similar data to those of  $^{32}\text{P}$ -GTP only. For the remaining wells, self-splicing reactions were performed in the presence of potential inhibitors. Data in Figure 3(A) can also be presented as a percentage of self-splicing reactions in the absence or presence of added compounds. The difference between the mean values of column 1 and column 12 serves as the common denominator in calculating the regulatory effect as a percentage. In Figure 3(B), the percentage

(A)

well	no compounds	with compounds										background
	1	2	3	4	5	6	7	8	9	10	11	12
A	8122	8146	7543	7033	6934	6016	6438	7502	6752	6905	7406	1767
B	7996	8281	7294	7762	6437	5861	6428	6782	6986	6839	4879	1331
C	7846	7429	6887	5663	6180	5736	5931	5716	5392	6406	5079	1397
D	7510	6800	6401	5542	5695	5530	5779	4974	5032	6098	6446	1577
E	7738	6634	5208	5462	5370	5115	4970	4740	5126	5534	5485	1497
F	7073	7120	5040	5486	4943	4882	2220	4971	5297	5617	5759	1386
G	7114	7571	6615	8564	3255	5689	5429	5868	6026	9442	6827	1792
H	6742	6466	6052	5843	5297	5751	5480	5392	4992	5797	5706	1547

(B)

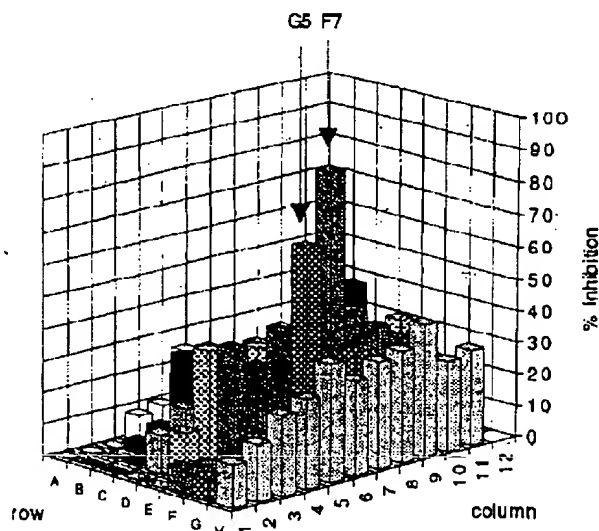


Figure 3. (A) An example of high-throughput screening data from the filtration assay. The value in each cell (or well in a 96-well microtiter plate) represents the radioactivity (in cpm) retained on the filter member. Column 1 represents the self-splicing reactions without any added compounds and column 12 represents background values obtained with samples containing  $^{32}$ P-GTP alone. In columns 2-11, each well represents the splicing reactions in the presence of a unique sample. Compared to values of column 1, a reduced value is expected if the self-splicing is inhibited. (B) Inhibition data expressed as the percentage inhibition of the self-splicing reactions (see text). A three-dimensional bar chart is used to represent the percentages of inhibition. The x-y plane indicates the location of each well and the z-axis indicates the percentage of inhibition. Wells (F7 and G5) that exhibit greater than 50% inhibition (marked by arrows) are readily identified.

in each well was obtained by subtracting the means of column 12 from the raw data in each well and then dividing this value by a common denominator. In this example, samples in wells F7 and G5 demonstrated an inhibitory effect greater than 50%. The eight repeats in column 1 (or column 12) suggest that there may be up to 20% error associated with this filtration assay. This should not affect the usage of this filtration method as a primary screening assay if the high-throughput screen is to quickly identify significant positive or negative effects in a large collection of compounds. The results of 18 plates (a total of 1440 samples) have been analyzed and the statistical distribution of the inhibitory activities is shown in Figure 4. This analysis is useful to optimize the screening conditions and to determine the selection of inhibitors from high-throughput screening.

The filtration method described here is useful as a primary assay for screening a large collection of compounds. Compounds that modulate (either up- or down-regulate) self-splicing reactions can be readily

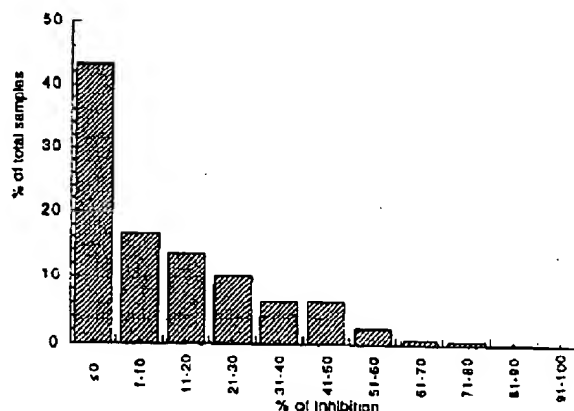


Figure 4. A statistical analysis of the inhibition data of the filtration assay. Out of 1440 samples tested, less than 5% of all the samples inhibit 50% of the self-splicing reactions of the *P. carinii* group I intron RNA.

identified by comparing the relative amount of products versus starting materials in the control samples. For example, in Figure 3, compared with wells containing control samples (column 1), a  $\approx 90\%$  decrease in radioactivity was observed for well F7. This indicates that samples in well F7 strongly inhibit the self-splicing reactions catalyzed by *P. carinii* group I introns.

Using this protocol, a compound library of  $\approx 150,000$  compounds was screened for inhibitors. Automation using a robotic workstation was employed to handle all the liquid samplings. Within three months, the entire compound library was screened at one single concentration for each compound.

The use of this filtration assay for high-throughput screening was supported by the findings that known inhibitors for group I introns were active in this assay. In our compound library, analogues of known self-splicing inhibitors such as guanosine and aminoglyco-

side antibiotics existed and were identified from the primary screen. After the initial screening, more than 1000 small organic molecules were identified to inhibit the self-splicing reactions catalyzed by *P. carinii* group I introns. The structures of three identified inhibitors are shown in Figure 5. Compounds 1, 2, and 3 represent three distinct, non-nucleic acid, non-aminoglycoside-based inhibitors for self-splicing group I introns. As shown in Figure 6, these compounds exhibit their inhibitory effects as a function of drug concentration with  $IC_{50}$  values around  $10\ \mu\text{M}$ . Under similar conditions, guanosine (nonradioactive) exhibits an  $IC_{50}$  value of  $0.2\ \mu\text{M}$ . Although the mechanism of inhibition may vary, these examples indicate that structurally different modulators for self-splicing group I intron RNA can be identified from a compound library using this filtration method.

In addition to the filtration method, a high-throughput gel electrophoresis assay with multiple loading capability has also been developed for studying self-splicing group I introns. To be specific, the reaction sample, prepared similarly to that described in the filtration assay, was loaded on a denaturing polyacrylamide gel (7 M urea, 6% polyacrylamide) and electrophoresed for 1 h at room temperature. Due to their lengths, the  $^{32}\text{P}$ -labeled products of the self-splicing introns can be readily distinguished from the  $^{32}\text{P}$ -GTP on a polyacrylamide gel. As previously shown in Figure 2(B), only 439-nt RNA (from the first step) and 390-nt RNA (from the second step), are observed on the gel. Under the applied electrophoresis conditions, free  $^{32}\text{P}$ -GTP did not interfere with the migration of any large RNA fragments from subsequent loadings and always ran out of the gel. On a single polyacrylamide, three or four repetitive loadings of different samples into the same wells at discrete times presented no interference between samples. Figure 7 shows the autoradiograph of a polyacrylamide gel (dimensions  $15 \times 15\ \text{cm}$ ) on which 20 different samples were loaded onto a single well at time 0, 1, and 2 h after the gel electrophoresis began. After 3 h of electrophoresis, the desired

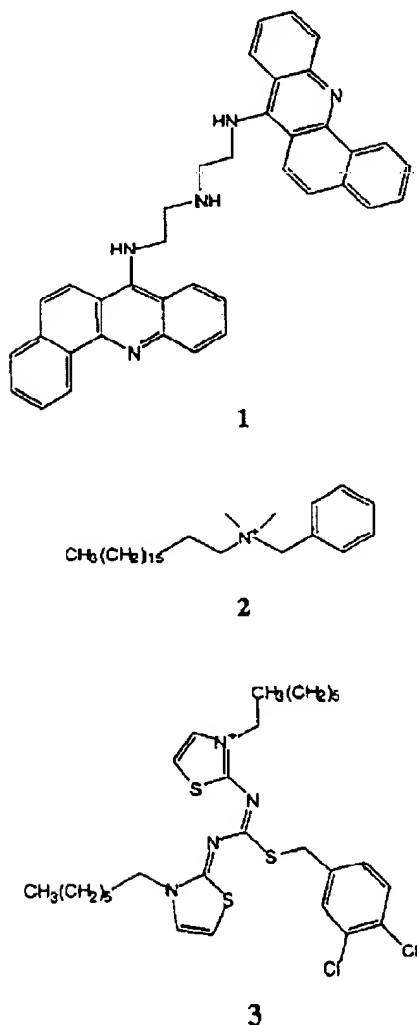


Figure 5. The structures of three self-splicing inhibitors: 1, 2, and 3.

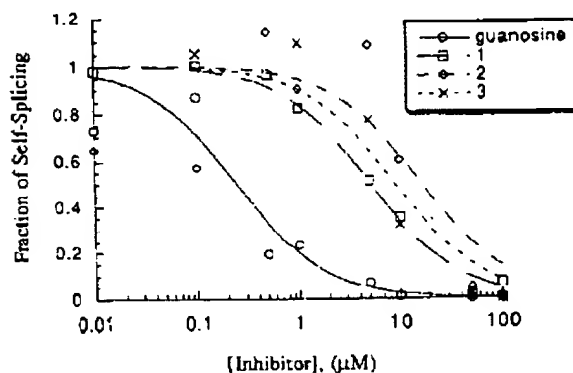
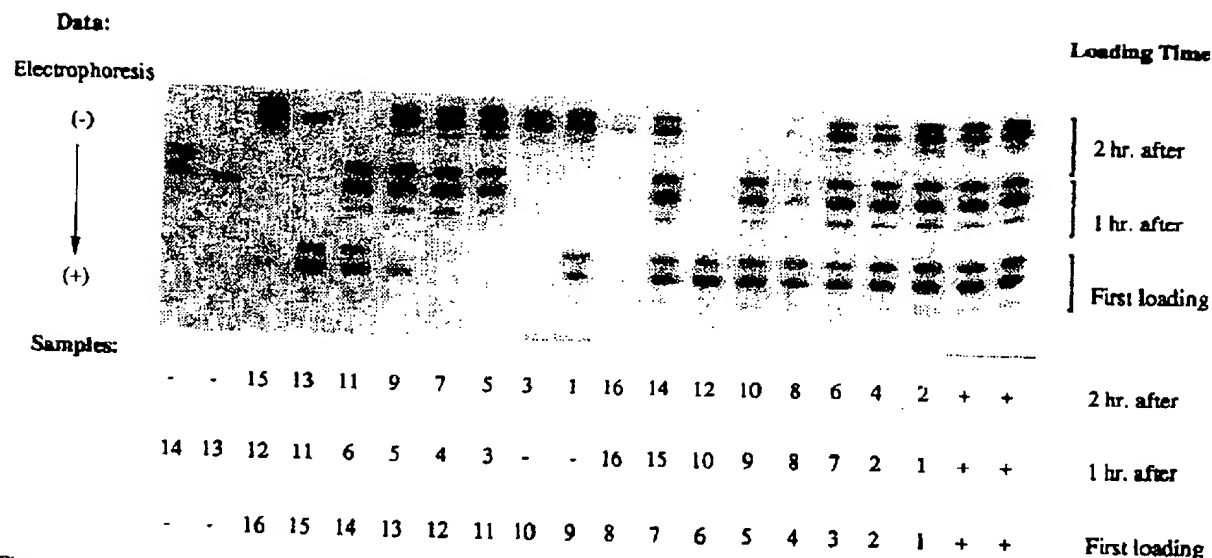


Figure 6. Titration studies of guanosine, 1, 2, and 3 using the filtration assay. All samples show dose-dependent inhibitory effect on self-splicing reactions. The  $IC_{50}$  value for guanosine is  $0.2\ \mu\text{M}$ ; for 1,  $5\ \mu\text{M}$ ; for 2,  $20\ \mu\text{M}$ ; for 3,  $9\ \mu\text{M}$ .



**Figure 7.** An example of multiloading gel electrophoresis assay for the self-splicing *P. carinii* group I intron RNA. On a polyacrylamide gel, the same 20 samples were loaded at three different times. Within each round of loading, the loading order (indicated at the bottom) for the 20 samples (from right to left) was different. Self-splicing reactions of *P. carinii* precursor RNA present two intense RNA bands on the gel. Inhibition of the self-splicing reactions is indicated by the decreased intensity of these two bands. Inhibition in samples 8, 10, 11, 12, 13, and 16 were observed regardless of when or where they were loaded.

products were well resolved in all of the samples regardless of the time of loading. Each sample contains the same self-splicing reaction solution as described in the previous section (32  $\mu$ L of precursor RNA in self-splicing buffer, 2  $\mu$ L of DMSO alone or compound in DMSO, and a 6  $\mu$ L solution of  $\alpha$ - $^{32}$ P-GTP).

To verify the validity of this multiple loading technique, the sample order was varied at each of the loading times. As shown in Figure 7, the first loading follows the sequence (from right to left) of samples that contain self-splicing reactions with no inhibitors added (two lanes, labeled as '+'), self-splicing in the presence of compound 1, 2, ..., 16, (16 lanes, labeled as 1, 2, ..., 16), and two repeats of control samples containing  $^{32}$ P-GTP only (two lanes, labeled as '-'). At the second and third loadings, the order of samples loaded on the same gel were scrambled compared to those of the first loading. As shown in Figure 7, samples containing compounds 8, 10, 11, 12, 13, and 16 can be readily identified as inhibitors ('hits') regardless of when and where they were loaded. In this gel electrophoresis assay, for the purpose of quantitation of reaction yields, appropriate  $^{32}$ P-labeled RNA fragments can be introduced to each sample as an internal standard immediately prior to loading. The gels containing self-splicing products and internal standards were dried and quantitated using a phosphorimager (Phosphorimager, Molecular Dynamics). Although more laborious than the filtration assay, the gel electrophoresis method described here has been demonstrated to be useful in high-throughput screening with the group I intron ribozyme as a molecular target.

In general, there is a good correlation between the filtration and gel electrophoresis assays. The most active (or inactive) compounds can be readily identified in the filtration assay and verified by the gel electrophoresis method. The self-splicing inhibitory effects of 10

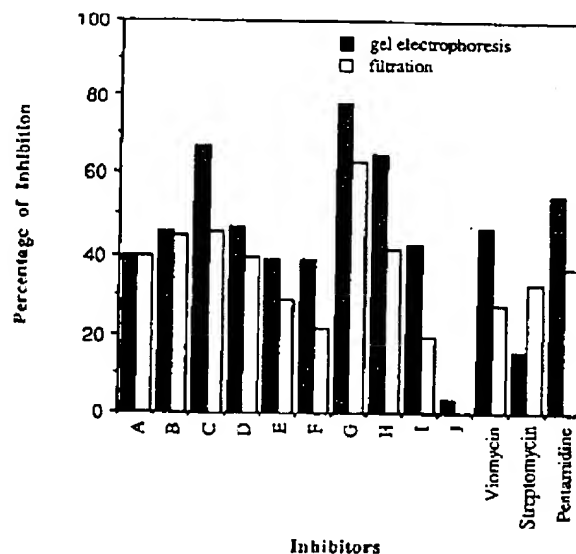


**Figure 8.** Correlation between the filtration and gel electrophoresis assays. Inhibition of self-splicing *P. carinii* group I intron RNA by 10 different compounds is shown. The inhibitory effects of compounds A-J obtained from filtration assay (open bars) were compared with those obtained from the gel electrophoresis method (hatched bars). As controls, inhibition data of viomycin, streptomycin, and pentamidine are also shown. In general, there is good correlation between the two assays.

compounds were examined using both the filtration assay and the gel electrophoresis method. In each sample, a single concentration (20  $\mu\text{M}$ ) of an inhibitor was prepared and aliquots were removed for either filtration or gel electrophoresis. Four repeats of each sample were performed and the average inhibition of each inhibitor was presented in Figure 8. Viomycin, streptomycin, and pentamidine, previously reported<sup>17</sup> as group I intron inhibitors at high  $\mu\text{M}$  concentrations, were also tested in both assays as controls. For example, compounds C and G were found to be the most active inhibitors in both filtration and gel electrophoresis assays. On the other hand, compound J was found to be inactive in both assays. Under similar conditions, viomycin, streptomycin, or pentamidine exhibited either low or modest activity.

Since the self-splicing assays described above include no nucleic acids other than the target ribozymes, the specificity of the identified inhibitors remains to be determined. If the inhibition is performed in the presence of a large excess of carrier DNA or RNA, nonspecific nucleic acid binders such as certain intercalators can be distinguished based on their reduced activity. However, similar activity should be found if the inhibition is specific for group I intron RNA. For example, the specificity of inhibitors 1–3 was evaluated in self-splicing reactions using 30  $\mu\text{M}$  nonradioactive *P. carinii* precursor RNA and 3  $\mu\text{M}$   $^{32}\text{P}$ -GTP in the presence of carrier nucleic acids (300  $\mu\text{M}$  of calf thymus DNA and 300  $\mu\text{M}$  of yeast tRNA<sup>Phe</sup>; all concentrations are in nucleotides). The presence of carriers affects the inhibitory effects of all three samples (data not shown). The  $\text{IC}_{50}$  values of these samples were five- to 10-fold higher than those in the absence of any carriers.<sup>18</sup> These data indicate that, in addition to affecting the self-splicing group I introns, compounds 1–3 may be mostly involved in nonspecific interactions with any nucleic acids. Under similar conditions, the inhibition by guanosine was not affected by the addition of carriers.

We have also established an additional specificity study based on the T7 polymerase transcription method. As previously shown in Figure 2(B), two different biochemical reactions—self-splicing and in vitro transcription—occurred in the same reaction mixture containing high concentrations of GTP and double-stranded DNA templates for RNA synthesis. The specificity is determined if the inhibitor affects only the self-splicing but not the transcription. In this assay, compounds of interest are added to the transcription buffer before any transcription or self-splicing is initiated. Figure 9 shows an example of this specificity study. The tested inhibitor was previously identified from the high-throughput filtration assay and verified by the gel electrophoresis method in the presence of carrier nucleic acids. The  $\text{IC}_{50}$  values of this inhibitor in both of these assays are  $\approx 1 \mu\text{M}$ . As shown in Figure 9, at a concentration of about 5  $\mu\text{M}$  this inhibitor blocked most of the self-splicing reaction without affecting the transcription of precursor RNA. The results obtained from high-throughput screening and selectivity studies demon-

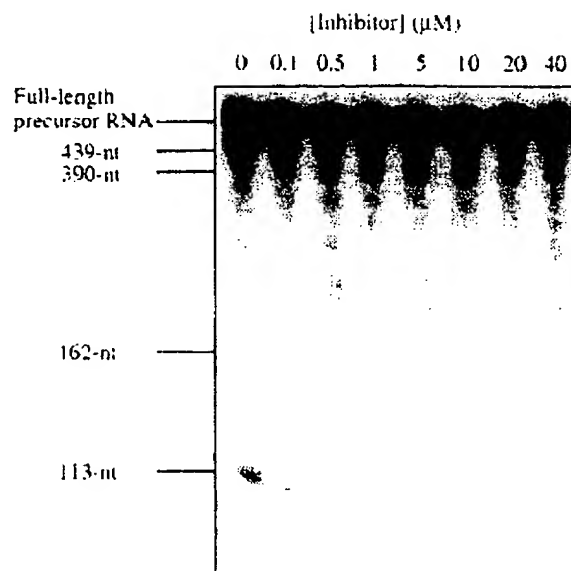


Figure 9. T7 in vitro transcription assay as a tool to evaluate the specificity of the self-splicing inhibitors. A self-splicing inhibitor identified from the filtration and gel electrophoresis method was tested in this assay. This compound inhibits the self-splicing reactions but not the transcription of *P. carinii* precursor RNA.

strated the utility of our mass-screening approach. Both the in vitro transcription assay and the gel electrophoresis assay in the presence of a large excess of carrier nucleic acids have been used as secondary screens. These assays have been used to evaluate the selectivity of the inhibitors identified from the primary filtration screen and their priorities for further drug development.

Furthermore, the nature of small-molecule inhibition of self-splicing group I introns can be determined from mechanistic studies. Basic principles and equations applied to regular enzymes can also be used in self-splicing ribozyme systems with certain modification. Unlike normal enzymes, the concentration of group I intron ribozyme decreases as the self-splicing proceeds. Therefore, the self-splicing ribozyme does not have any turnover and the maximum velocity occurs only at the initial time.<sup>19</sup> With these considerations, a Michaelis-Menten mechanism can be applied to estimate kinetic parameters such as  $K_m$ ,  $k_{cat}$ , and  $K_i$  of the self-splicing reactions.<sup>19</sup> The kinetic studies can be performed using either internally labeled or end-labeled precursor RNA as the starting material (Fig. 2B). The relative amounts of the full-length precursor RNA and the spliced products can be quantitated and calculated to obtain the efficiency of the self-splicing reactions. Mechanistic studies of certain inhibitors are currently underway to understand the details of their mechanism of action and to design better inhibitors.

# A ligation reaction catalyzed by a self-assembled ribozyme derived from *sunY* group I introns

We have recently screened for small-molecule inhibitors of another ribozyme system derived from self-splicing group I introns. As shown in Figure 1(A), the well-defined catalytic core of group I intron includes conserved sequences P, Q, R, S, a G/C base pair as the binding site for guanosine, and the P1 and P10 segments containing the 5' and the 3' splice sites, respectively. There has been an increasing number of chemical reactions found to be catalyzed by ribozymes derived from group I introns.<sup>2</sup> The activities found for the group I introns include that of a ribonuclease,

phosphotransferase, acid phosphatase, DNA or RNA restriction endonuclease, RNA ligase, RNA polymerase, and aminoacyl esterase. Most interestingly, all of these reactions seem to use the same catalytic domain for biocatalysis.

RNA fragments containing P, Q, R, and S sequences have been demonstrated to assemble and form a multisubunit ribozyme that catalyzes an RNA ligation reaction.<sup>14</sup> As shown in Figure 10(A), this self-assembled ribozyme system is composed of three RNA fragments: 59 nt, 43 nt, and 36 nt. It has been demonstrated that this ribozyme, in the presence of  $Mg^{2+}$ , catalyzes the ligation of a 6-nt RNA fragment to a

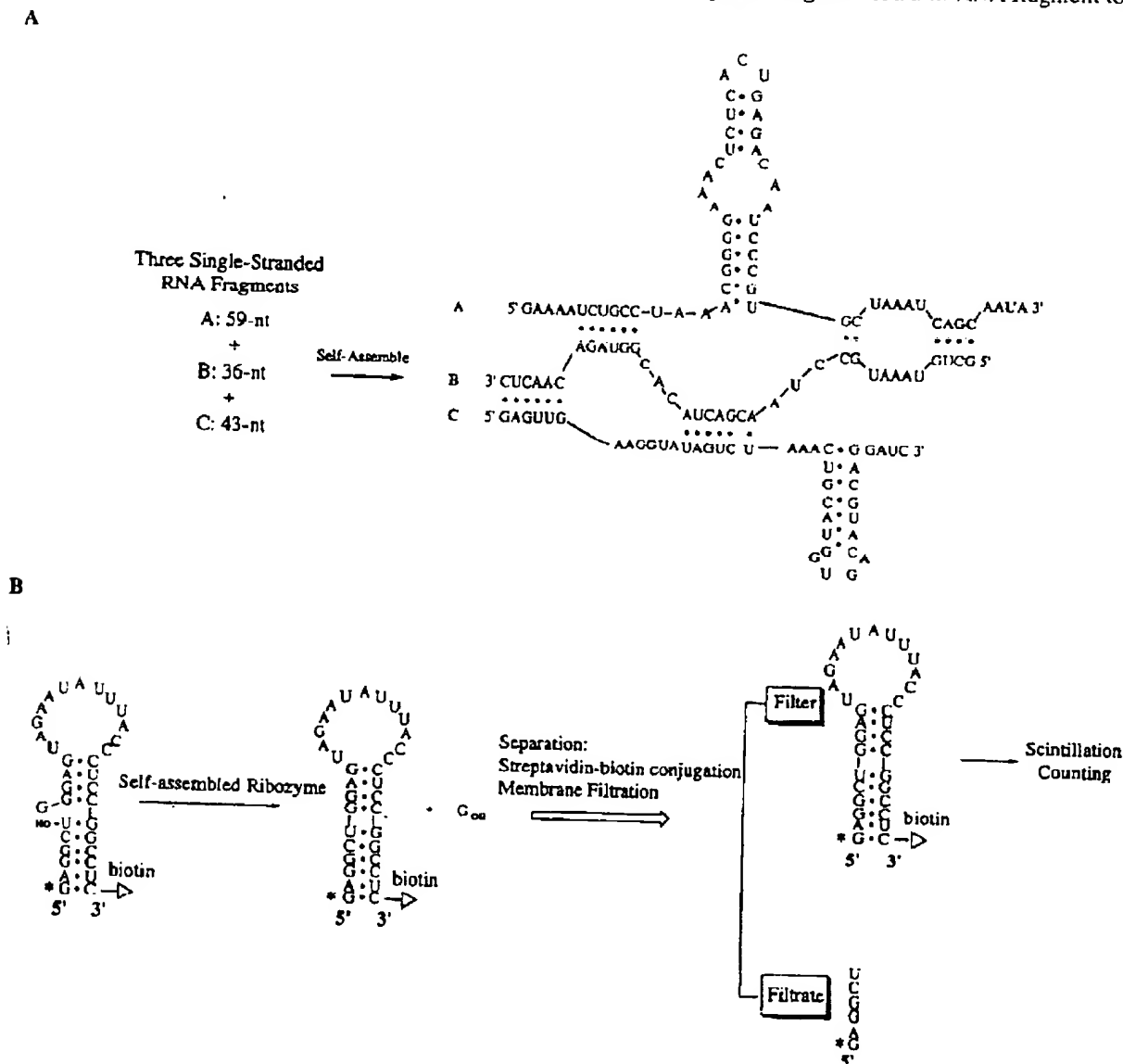


Figure 10. (A) The formation of a self-assembled ribozyme system from three RNA fragments. (B) The RNA ligation reaction catalyzed by the self-assembled ribozyme system. The given example uses a separation procedure including the streptavidin-biotin conjugation and membrane filtration to separate the  $^{32}P$ -six-nt RNA (starting material) and the 5'- $^{32}P$ , 3'-biotin-33-nt RNA (ligation product). The radioactivity retained on the filters is determined by scintillation counting. This value indicates the extent of ligation reaction catalyzed by the self-assembled ribozyme.



28-nt RNA (Fig. 10B). The assembled ribozyme catalyzes the nucleophilic attack of the 3'-OH from the 6-nt to the 3'-phosphodiester linkage following the 5'-guanine residue of the 28-nt RNA. The products include a guanosine released from the 28-nt RNA and a ligated 33-nt RNA product. This ligation reaction represents a mimicry of either the reversal of the first step in the group I intron self-splicing process or simply the second reaction. Regulation of this self-assembled ribozyme system may serve as a model for modulating any other biological reactions catalyzed by the group I intron RNA.

A high-throughput filtration assay capable of screening compounds that regulate the RNA ligation reaction catalyzed by the self-assembled ribozyme system has now been established. This assay includes the use of radioisotope (e.g.,  $^{32}\text{P}$ ) labeling at the 5'-end of the 6-nt RNA substrate and the incorporation of a biotin molecule at the 3'-end of the 28-nt RNA substrate. The ligation reaction catalyzed by the self-assembled ribozyme system shown in Figure 10(B) was designed to generate a 5'- $^{32}\text{P}$ , 3'-biotinylated 33-nt RNA product which can be readily distinguished from all the other RNA components in the mixture. To facilitate the separation of the 33-nt product from the 6-nt RNA, a protocol of biotin-streptavidin conjugation<sup>29</sup> is incorporated into this assay. The relative amounts of the  $^{32}\text{P}$ -labeled 6-nt and 33-nt product can be determined by the radioactivity retained on the filter membrane. The 33-nt biotinylated products conjugated with streptavidin will remain on the filter while free  $^{32}\text{P}$ -6-nt will pass through during filtration. The biotinylated 28-nt RNA substrate itself is not radiolabeled. Therefore, when it is conjugated with added streptavidin, it does not interfere with product analysis. Compounds that regulate (either up- or down-regulate) the designed ligation reactions are identified by their differential radioactivity retained on the filter compared with the control sample, which contains no compounds.

The results obtained from this high-throughput assay in a 96-well microtiter plate are shown in Figure 11(A). Percentage inhibition of the ligation reaction in the absence or presence of added compounds can be obtained from the raw data as described in the previous section. Column 1 represents the results of the ligation reactions catalyzed by the self-assembled ribozyme in the absence of any inhibitors while column 12 represents the data of the solution containing RNA substrates ( $^{32}\text{P}$ -6-nt and 28-nt) only. Other control experiments, such as ribozyme-catalyzed ligation reaction at time zero, showed data similar to those of RNA substrates only. As shown in Figure 11(A), compared to control samples, decreased radioactivity found in certain wells (e.g., A3, A7, and A9) indicates ligation is inhibited by the presence of compounds. In theory, compounds that up-regulate the catalysis can also be identified by the increased counts in radioactivity.

An alternative method of separation and detection is the use of scintillation proximity assay (SPA).<sup>21</sup> In the

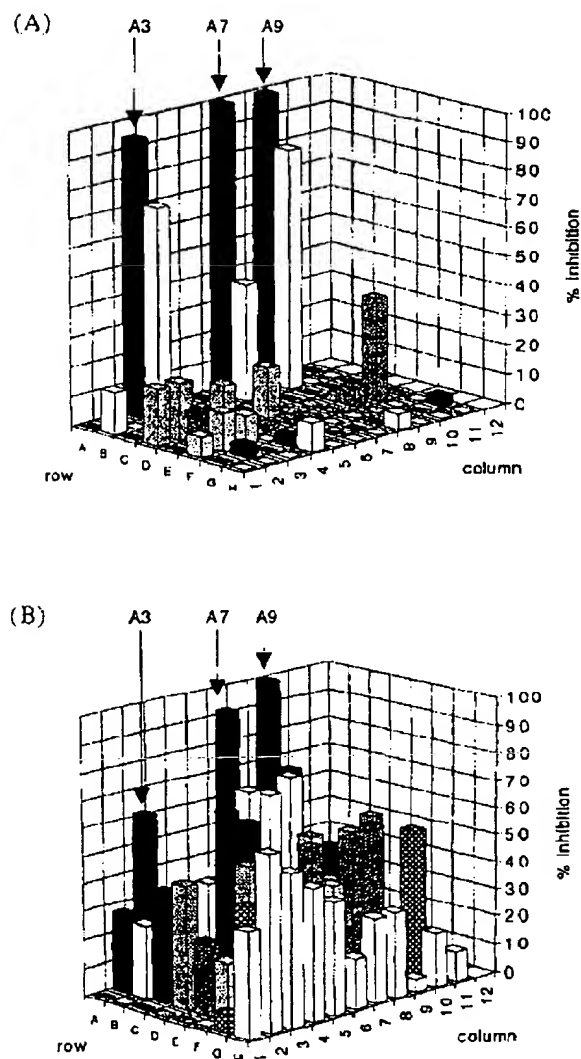


Figure 11. (A) An example of high-throughput screening data from the self-assembled ribozyme system using the filtration assay. In columns 2-11, each well represents the ligation reaction in the presence of a unique sample. Similar to Figure 3(B), the z-axis indicates the extents of inhibition in the presence of different samples. (B) Inhibition data obtained for the same sample plate using SPA. As indicated by arrows, most active wells (A3, A7, and A9) are evident in both assays.

ligation experiment described above, the final product, 33-nt ligated RNA, is biotinylated and can be immobilized on the SPA beads through biotin-streptavidin conjugation. If the RNA is labeled with 'weak'  $\beta$  particle-emitting isotopes such as  $^{33}\text{P}$ ,  $^{35}\text{S}$ , and  $^3\text{H}$ , the efficiency of ribozyme-catalyzed ligation can be followed by the light emitted from the scintillant embedded in the SPA beads. This detection method eliminates the separation procedure and significantly simplifies the screening assay. Figure 11(B) shows SPA data obtained for the same sample plate previously studied by the filtration method. By comparing the data of Figure 11(A) and (B), samples in wells such as A3,

A7, and A9 were found to be active regardless of the separation method used. Discrepancies in the data of certain wells may be due to the different natures of these assays. The error observed for the SPA method was slightly higher.

Current studies focus on the intron sequence obtained from *P. carinii* or phage T4. Inhibitors that function through a mechanism common to group I introns in *P. carinii* or phage T4 could have the potential to block similar self-splicing reactions in other group I intron systems. Investigations into this hypothesis are in progress in our laboratory.

### Summary

Methods that are amenable for automation or high-throughput screening have been developed to identify small organic molecules that regulate (activate or suppress) the activity of a particular ribozyme. Methods of labeling of nucleic acids (with radioactive isotopes, fluorescent tags, or biotin) and separation of starting material and final products (using filtration, gel electrophoresis, or biotin-avidin conjugation) are discussed. These methods are used to separate and quantitate the reactants and the products and to evaluate the effects of small molecules on the chemical reactions catalyzed by ribozymes of interest. The *in vitro* assays discussed here include no proteins or other macromolecular targets other than ribozymes. The low molecular weight organic modulators thus identified must interact directly with ribozyme molecules. In addition to the examples provided, these methods should be applicable to a variety of ribozyme, or even enzyme, systems derived from DNA molecules.

Although yet to be proven, inhibitors following this specific mechanism could be of clinical utility in treating or detecting infections caused by microorganisms whose life cycle is regulated by the catalytic function of group I introns. If such agents are shown to be clinically useful, then *in vitro* assays described here might be more generally used to screen agents targeting a variety of RNA-catalyzed reactions. The cellular or *in vivo* activities of the identified self-splicing inhibitors are the subject of current investigation.

### Experimental

#### Materials

Unless otherwise mentioned, all biochemicals were obtained from Sigma and used without further purification. The compound library of Parke-Davis was used for high-throughput screening against the *P. carinii* group I introns or the self-assembled ribozyme.

#### Preparation of *P. carinii* precursor RNA

The 552-nt precursor RNA—including a 489-nt sequence derived from *P. carinii* Ss-rRNA, a short 5'-fragment, and a 3'-overhang sequence—was prepared as described previously with some modification.<sup>15</sup> The 489-bp sequence of cDNA encoding a 390-nt group I intron sequence, a 68-nt 5' exon, and a 31-nt 3'-exon was prepared by PCR reaction using six overlapping oligonucleotides ( $\approx 100$  nt each, chemically synthesized) and two primer sequences. The PCR amplified products were cloned into a pGEM-4Z vector (Promega) previously linearized by *Sma* I. The vector was transfected into *E. coli* and the clones containing the 489-bp cDNA were verified by enzyme digestion and dideoxy sequencing. The correct pGEM constructs were linearized with *EcoR* I and used as a template for *in vitro* transcription with T7 RNA polymerase. When necessary, the 552-nt RNA transcripts were purified by polyacrylamide gel electrophoresis.

#### Preparation of the self-assembled ribozyme systems

All RNA fragments were chemically synthesized using phosphoramidite chemistry and purified by PAGE. Biotinylated 28-nt RNA was synthesized using CPG supports containing biotin at the 3'-terminus (BioTEG-CPG, Glen Research). 6-nt RNA was phosphorylated using T4 polynucleotide kinase and [ $\gamma$ -<sup>32</sup>P] ATP (Amersham).

#### High-throughput filtration assay for *P. carinii* group I introns

In each well of a 96-well U-bottom microtiter plate, 32  $\mu$ L of precursor RNA (in self-splicing buffer 50 mM Tris-HCl, pH 7.5, 10 mM (NH<sub>4</sub>)<sub>2</sub>SO<sub>4</sub>, 10 mM MgCl<sub>2</sub>, 5 mM spermidine, and 5% glycerol) was added to 2  $\mu$ L of small organic compounds (in DMSO) and the mixture was incubated at room temperature for 5 min. This incubation ensures pre-equilibration between the enzymes and the inhibitors before the addition of a 6  $\mu$ L solution of  $\alpha$ -<sup>32</sup>P-GTP ( $\approx 10,000$  cpm in self-splicing buffer) to initiate the self-splicing reaction. The final concentration of the precursor RNA was 50 nM (in molecules). The reaction mixture was incubated at 50 °C for 3 h before 150  $\mu$ L of 11% aqueous trichloroacetic acid (TCA) was added to stop the splicing reactions and to precipitate the RNA. The TCA/reaction mixture was incubated at room temperature for 5 min and transferred to a nitrocellulose filter plate (Millipore, MHAB, pretreated with 100  $\mu$ L of 0.05% polyethyleneimine for 15 min). Filtration was performed on a vacuum manifold (Millipore, MAVM) and the filter membrane was washed once with 200  $\mu$ L of washing buffer (0.1 N HCl, 100 mM Na<sub>2</sub>P<sub>2</sub>O<sub>7</sub>). The filter was allowed to dry and the retained radioactivities were determined using scintillation counting (Wallac Microbeta Counter). Due to the use of the 96-well microtiter plates, all solution handling was automated by using a robotic workstation (Beckman, Biomek 1000).

### High-throughput filtration assay for the self-assembled ribozyme system

The assay was performed in 96-well microtiter plates. To each well, 48  $\mu$ L of the three-fragment ribozyme solution (in 30 mM Tris-HCl, pH 7.5; 150 mM MgCl<sub>2</sub>; 10 mM NH<sub>4</sub>Cl; 400 mM KCl; 10% polyethyleneglycol, annealed at 55 °C for 10 min then cooled down to 37 °C gradually) was added to 3  $\mu$ L of compounds in DMSO (final concentration of 20  $\mu$ M). The mixture was equilibrated at room temperature for 5 min and 9  $\mu$ L of the substrate RNA solution was added. The final concentration (in molecules) of the ribozyme was 50 nM; of the 28-nt substrate, 20 nM; and of the 6-nt substrate,  $\approx$ 100 pM ( $\approx$ 10,000 cpm). The reaction was incubated at 37 °C for 2 h and stopped by the addition of 180  $\mu$ L of an 8 M urea/formamide solution (2:1 volume ratio). We found that the addition of urea/formamide solution significantly reduced the amount of nonspecific binding of unligated RNA substrates to streptavidin-coated SPA beads. After 5 min of mixing and standing, aliquots (120  $\mu$ L) of the mixture were transferred to a 96-well filtration plate (Millipore, MHA8) pre-wet with cold washing buffer (e.g., 10 mM phosphate, pH 7.2 and 1.15 M NaCl, 0.05% NaN<sub>3</sub>, and 5% glycerol). A 100  $\mu$ L solution of streptavidin-coated SPA beads (Amersham International, 0.625 mg/mL in washing buffer) was added to each well. After equilibrating for a further 10 min, filtration was performed using a Multiscreen Vacuum Manifold (Millipore). The filters were washed with cold washing buffer once and dried before determining their radioactivities using a Wallac Microbeta Liquid Scintillation Counter.

### References

- Cech, T. R. *Gene* **1993**, *135*, 33.
- (a) Cech, T. R. *Bio/Technology* **1995**, *13*, 323. (b) Altman, S. *Bio/Technology* **1995**, *13*, 327.
- Christoffersen, R. E.; Marr, J. J. *J. Med. Chem.* **1995**, *38*, 2023.
- von Ahsen, U.; Davies, J.; Schroeder, R. *Nature (London)* **1991**, *353*, 368.
- Cech, T. R. *Annu. Rev. Biochem.* **1990**, *59*, 543.
- Michel, F.; Westhof, E. *J. Mol. Biol.* **1990**, *216*, 585.
- Saldanha, R. J.; Patel, S. S.; Surendran, R.; Lee, J. C.; Lambowitz, A. M. *Biochemistry* **1995**, *34*, 1275.
- Taylor, J. *Annu. Rev. Microbiol.* **1992**, *46*, 253.
- Liu, Y.; Leibowitz, M. J. *Nucleic Acids Res.* **1995**, *23*, 1284.
- (a) Bass, B. L.; Cech, T. R. *Biochemistry* **1986**, *25*, 4473. (b) Yarus, M. *Science* **1988**, *240*, 1751.
- von Ahsen, U.; Davies, J.; Schroeder, R. *J. Mol. Biol.* **1992**, *226*, 935.
- The therapeutic application of ribozyme inhibitors of peptide, nucleic acid, or aminoglycoside-like molecules have been reported previously in: (a) Cech, T. R. (1991) PCT Int. Appl. 38 pp. CODEN: PIXXD2. WO 9106302 A1 910516. (b) von Ahsen, U.; Davies, J.; Schroeder, R. (1993) PCT Int. Appl. 18 pp CODEN: PIXXD2. WO 9300907 A1 930121.
- Lin, H.; Niu, M. T.; Yoganathan, T.; Buck, G. A. *Gene* **1992**, *179*, 163.
- Doudna, J. A.; Couture, S.; Szostak, J. W. *Science* **1991**, *256*, 1605.
- Barrett, J. F.; Ohemung, K. A. *Expert Opin. Invest. Drugs* **1994**, *3*, 303.
- For the sake of clarity, we did not distinguish the two longer RNA products (5'-guanine-439-nt and 5'-guanine-390-nt) from their original RNA fragments. Regardless of the incorporation of a guanosine, 439-nt and 390-nt were always used to represent these two RNA fragments, respectively.
- (a) Wank, H.; Rogers, J.; Davies, J.; Schroeder, R. *J. Mol. Biol.* **1994**, *236*, 1001. (b) Liu, Y.; Tidwell, R. R.; Leibowitz, M. J. *J. Euk. Microbiol.* **1994**, *41*, 31.
- Similar splicing experiments were performed using 30 nM of 5'-<sup>32</sup>P-labeled *P. carinii* precursor RNA and 3  $\mu$ M cold GTP in the presence of 300  $\mu$ M of carrier calf thymus DNA and yeast tRNA<sup>phe</sup>. The effects of carriers on the inhibitory activities of compounds 1-3 were not significant. Compared to the data obtained using nonradioactive precursor RNA, the discrepancy might result from the different conditions of these experiments.
- Bass, B. L.; Cech, T. R. *Nature (London)* **1984**, *308*, 820.
- Green, N. M. In *Methods in Enzymol.*; Bayer, E. A.; Wilchek, M., Eds; Academic: **1990**; Vol. 184, p 51.
- Uderfriend, S.; Gerber, L.; Nelson, N. *Anal. Biochem.* **1987**, *161*, 494.

(Received in U.S.A. 14 October 1996; accepted 18 February 1997)